1,2-Diacyl-Phosphatidylcholine Flip-Flop Measured Directly by Sum-Frequency Vibrational Spectroscopy

Jin Liu and John C. Conboy
Department of Chemistry, University of Utah, Salt Lake City, Utah

ABSTRACT Sum-frequency vibrational spectroscopy (SFVS) is used to measure the intrinsic rate of lipid flip-flop for 1,2-dimyristoyl-*sn*-glycero-3-phosphocholine (DMPC), 1,2-dipalmitoyl-*sn*-glycero-3-phosphocholine (DPPC), and 1,2-distearoyl-*sn*-glycero-3-phosphocholine (DSPC) in planar-supported lipid bilayers (PSs). Asymmetric PSLBs were prepared using the Langmuir-Blodgett/Langmuir-Schaefer method by placing a perdeuterated lipid analog in one leaflet of the PSLB. SFVS was used to directly measure the asymmetric distribution of the native lipid within the membrane by measuring the decay in the CH_3 ν_s intensity at 2875 cm^{-1} with time and as a function of temperature. An average activation energy of 220 kJ/mol for the translocation of DMPC, DPPC, and DSPC was determined. A decrease in alkyl chain length resulted in a substantial increase in the rate of flip-flop manifested as an increase in the Arrhenius preexponential factor. The effect of lipid labeling was investigated by measuring the exchange of 1,2-dipalmitoyl-*sn*-glycero-3-phosphoethanolamine-*n*,*n*-Dimethyl-*n*-(2′,2′,6′,6′-tetramethyl-4′-piperidyl) (TEMPO-DPPC). The rate of TEMPO-DPPC flip-flop was an order-of-magnitude slower compared to DPPC. An activation energy of 79 kJ/mol was measured which is comparable to that previously measured by electron spin resonance. The results of this study illustrate how SFVS can be used to directly measure lipid flip-flop without the need for a fluorescent or spin-labeled lipid probe, which can significantly alter the rate of lipid translocation.

INTRODUCTION

A central issue in molecular biology is the movement of lipids across the cellular membrane, otherwise known as lipid *flip-flop* or *translocation*. The translocation of lipids is involved in cell apoptosis, the viral infection of living cells, and the functioning of antibiotics, antiseptics, and drugs. As the biogenesis of lipid occurs on the cytosolic side of the membrane, the outer membrane must also be continually supplied with new lipid species by lipid translocation if cell growth is not to be hindered. There is a growing body of evidence that the exchange of lipids between the inner and outer leaflets of cellular membranes occurs by a protein-mediated process (1–11). The measured transport of lipids in the endoplasmic reticulum (ER) is fast, with half-lives on the order of minutes (2,3,12–16). Studies of lipid flip-flop using reconstituted membrane lipids and proteins of the ER have shown facile exchange of lipids under physiological conditions. The exchange was found to be independent of the glycerolphospholipid headgroup identity and is independent of ATP, suggesting that active transport is not required (2,13,15–16). There have also been a number of studies performed on reconstituted bacterial cytoplasmic membranes, showing similar behavior (17,18). In contrast to lipid transport in the ER, the movement of lipids in the plasma membrane of eukaryotic cells appears to be dependent upon some stimulus, and has been suggested to be headgroup-selective and possibly unidirectional (6,19–21). These observations have been driven in large part by the observation of highly asymmetric lipid compositions in the inner and outer leaflets of the plasma membrane. Several putative protein *flipases* or *flopases* have been identified, which might be responsible for lipid migration (1,16,20,22).

Studies on protein-free liposome model membrane systems using fluorescent or spin-labeled phospholipids have suggested a slow rate of migration, on the order of hours to days (8,23–25). These studies demonstrate that the transbilayer movement of lipids is possible in the absence of protein-mediated processes, but is usually too slow to be of biological importance. An activation barrier of ~81 kJ/mol has been calculated for a TEMPO-labeled phosphatidylethanolamine lipid in an egg phosphatidylcholine matrix by electron spin resonance (ESR) (24). The value measured from this study has been used repeatedly to justify the absence of free lipid migration. However, these studies only detected the movement of a labeled lipid, which contained significant chemical and structural differences compared to the native lipid species found in biological membranes.

The model membrane systems used to study lipid migration have predominately focused on lipid vesicles or liposomes (1,8,9,16,24,26–30). These solution-phase analogs of cell membranes are composed of a single spherical lipid bilayer with dimensions usually on the order of tens of nanometers to several microns. The most widely used analytical tools for investigating lipid flip-flop in these systems have been ESR and fluorescence spectroscopy. ESR and fluorescence require the use of spin-labeled analogs of naturally occurring lipids (usually a nitroxide radical group such as TEMPO) (24,25,31–36), or fluorescently-labeled lipid species (4,9,20,25,29,37–44). The direct measurement of lipid translocation with ESR or fluorescence, however, is not possible due to the inability to determine the location (inner or outer

Submitted May 3, 2005, and accepted for publication July 19, 2005.

Address reprint requests to John Conboy, E-mail: conboy@chem.utah.edu.

0006-3495/05/10/2522/11 $2.00

doi: 10.1529/biophysj.105.065672

leaflet) of the lipid probe in the membrane. For this reason, chemical modification or extraction of the lipids on the exterior of the liposome is required to produce an asymmetric distribution of lipids in the bilayer (4,29,45).

In addition to solution-phase model systems, planar-supported lipid bilayers (PSLBs) have been used extensively to study a variety of membrane processes including protein insertion/binding, structure, dynamics, and fluidity (46–56). Many methods for preparing supported lipid bilayers have been discussed in the literature. PSLBs are typically prepared by two distinct methods, either by the Langmuir-Blodgett/Langmuir-Schaefer (LB/LS) technique (46,55,57,58) or vesicle spreading (56,58–61). Vesicle spreading utilizes solution-phase liposomes which are fused to a solid support, typically a glass or fused silica substrate, resulting in the formation of a uniform bilayer-coated surface. Vesicle fusion, however, does not allow for control over the composition of the bilayer, in terms of the lipids present in the top or bottom leaflets or the lateral packing density. In contrast to vesicle fusion method, the LB/LS method can be used to prepare bilayer assemblies with a great amount of control of the lipid composition and structural arrangement of the bilayer. This key feature of LB/LS method allows asymmetric lipid assemblies to be created, which is extremely advantageous when examining lipid translocation.

One concern which is often voiced when PSLBs are used in membrane studies is the influence of the substrate on the membrane properties. Fluorescence recovery after photobleaching studies have shown that membrane fluidity in the upper and bottom leaflets of PSLBs on a silica surface are identical, within error according to the work of Wagner and Tamm (62), suggesting that there is no strong coupling of the bilayer to the substrate. In addition, the efficacy of these model membrane systems has been well established by a number of researchers (46–56).

To complement the ESR and fluorescence techniques discussed above, we have introduced a new method for directly measuring lipid transbilayer migration. The method uses the nonlinear spectroscopic technique of sum-frequency vibrational spectroscopy (SFVS) to directly measure the population inversion of lipids in a PSLB (63). SFVS is a coherent nonlinear optical vibrational spectroscopy. The coherent nature of SFVS makes the technique ideal for studying the asymmetry in a lipid bilayer, something which is not possible with linear spectroscopic methods including ESR, infrared (IR), and fluorescence. The theoretical foundations of SFVS have been well established in the literature and will not be thoroughly discussed here (64). SFVS is a second-order nonlinear optical spectroscopy, which has the chemical selectivity of IR and Raman and is inherently surface-specific in nature. Experimentally, SFVS is performed by overlapping, both spatially and temporally, a visible and tunable IR laser source on a surface where they combine to produce a third photon at the sum of their respective frequencies. The symmetry constraints on SFVS restrict this process to the interface, where the inversion symmetry of the bulk phases is broken, making the technique surface-specific (64). The intensity of the SFVS signal, I_{SF}, is given by

$$I_{SF} = \left| \tilde{f}_{SF} f_{vis} f_{ir} \chi^{(2)} \right|^2, \tag{1}$$

where $\chi^{(2)}$ is the second-order nonlinear susceptibility tensor, and $\tilde{f}_{SF}$, f_{vis}, and f_{ir} are the geometric Fresnel coefficients describing the local electric field intensities for the sum, visible, and IR beams, respectively (65,66).

The nonlinear susceptibility tensor, $\chi^{(2)}$, is the sum of a resonant (R) and nonresonant (NR) contribution given by

$$\chi^{(2)} = \chi_{NR} + \chi_R, \tag{2}$$

with the resonant contribution defined as

$$\chi_R = N\left(\sum_{x=1}^{m} \frac{\langle A_k M_{ij} \rangle_x}{\omega_{\nu_x} - \omega_{ir} - i\Gamma_{\nu_x}} \right), \tag{3}$$

where N is the number of molecules, m is the number of vibrational transition, A_k is the IR transition probability, M_{ij} is the Raman transition probability, ω_{ir} is the frequency of the input IR field, ω_ν is the normal mode vibrational frequency of the transition being probed, and Γ_ν is the linewidth of the transition. For a transition to be observed by SFVS, it must be both IR- and Raman-active. A sum-frequency spectrum is obtained by tuning the IR frequency through the vibrational resonance of the molecules comprising the interface and measuring the intensity of the resulting SF light. For the studies presented here, the C-H vibrational modes between 2800 cm^{-1} and 3000 cm^{-1} of the fatty acid chains of the lipids are examined.

The symmetry constraints imposed on SFVS, through the $\chi^{(2)}$ tensor (64), also provide a highly sensitive method for determining the asymmetry in lipid bilayers. Since SFVS is a coherent vibrational spectroscopy, the arrangement of the transition moments of the molecules comprising the interface has a dramatic effect on the measured response. Take, for example, the symmetric stretch (ν_s) of the terminal CH_3 groups on the lipid fatty acid chains of a typical phospholipid. The transition dipole moment lies along the C-C bond, as illustrated in Fig. 1. If another lipid chain is placed antiparallel to the first, in an arrangement found in a typical lipid bilayer, the sum of the two transitions will cancel each other due to the their opposing phases. The result is that no SFVS response will be observed from such an assembly.

As with IR spectroscopy, the components of a vibrational transition parallel or perpendicular to the surface can be examined by the proper polarization choice of the incident electric fields. For SFVS, transitions parallel to the surface normal are probed with the polarization combination of *s*-polarized sum-frequency, *s*-polarized visible, and *p*-polarized IR (*ssp*), whereas transitions perpendicular to the surface normal are measured with the *s*-polarized sum-frequency, *p*-polarized visible, and *s*-polarized IR (*sps*) polarization

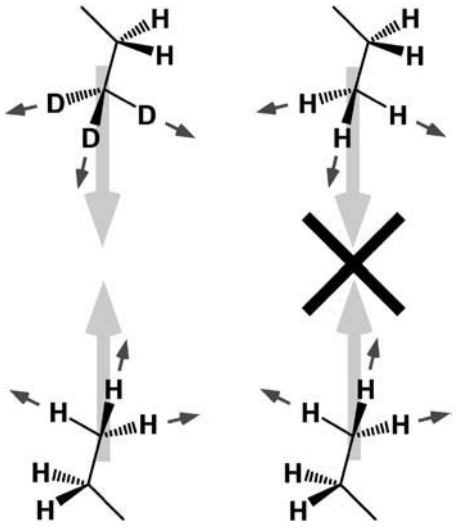

FIGURE 1 Absence of dipole cancellation for the CH_3 ν_s in an asymmetric bilayer with one leaflet containing CD_3 groups (*left*) and the illustration of the antiparallel arrangement of the transition dipole moments for the CH_3 ν_s in a pure lipid bilayer resulting in dipole cancellation (*right*).

combination. As we are interested in probing the asymmetry between the two leaflets of the lipid bilayer, the *ssp* polarization combination is used in this study.

For a lipid bilayer composed of identical lipids in the inner and outer leaflets, near-complete destructive interference of the vibrational resonances arising from the fatty acid chains of the lipids is observed due to their antiparallel orientation. By creating an artificially asymmetric structure in which a lipid monolayer is placed in contact with a deuterated lipid monolayer, changes in the membrane lipid composition due to exchange between leaflets can be followed directly by measuring the changes in the vibrational signatures of the alkyl chains with time. This methodology does not require the use of fluorescent or spin-labeled probes and the use of chemical agents to selectively destroy the population of probes on the outer membrane surface. In the study presented here, the dynamics of lipid flip-flop for three lipid species, 1,2-dimyristoyl-*sn*-glycero-3-phosphocholine (DMPC), 1,2-dipalmitoyl-*sn*-glycero-3-phosphocholine (DPPC), and 1,2-distearoyl-*sn*-glycero-3-phosphocholine (DSPC) in PSLBs are examined. The temperature dependence of flip-flop is measured and the activation free energy for native lipid translocation is calculated. These results are compared with the energetics of flip-flop for a TEMPO-labeled lipid to investigate the influence of headgroup modification on lipid migration.

EXPERIMENTAL

Materials

D_2O (99.9%) was purchased from Cambridge Isotope Laboratories (Andover, MA) and used without any further purification. GC grade $CHCl_3$ was supplied from Mallinckrodt (Mallinckrodt Baker Bioscience, Phillipsburg, NJ). 1,2-dimyristoyl-D54-*sn*-glycero-3-phosphocholine-1,1,2,2-D4-*n*,*n*,*n*-trimethyl-D9 (DMPC-d_{67}), 1,2-dipalmitoyl-D62-*sn*-glycero-3-phosphocholine-1,1,2,2-D4-*n*,*n*,*n*-trimethyl-D9 (DPPC-d_{75}), 1,2-distearoyl-D70-*sn*-glycerol-3-phosphocholine-1,1,2,2-D4-*n*,*n*,*n*-trimethyl-D9 (DSPC-d_{83}), 1,2-dipalmitoyl-*sn*-glycero-3-phosphoethanolamine-*n*,*n*-Dimethyl-*n*-(2′,2′,6′,6′-tetramethyl-4′-piperidyl) (TEMPO-DPPC), and the ammonium salt of 1,2-dipalmitoyl-*sn*-glycero-3-phosphoethanolamine-N-(7-nitro-2-1,3-benzoxadiazol-4-yl) (NBD-DPPE) were purchased from Avanti Polar Lipids (Alabaster, AL) as either lyophilized powders or in $CHCl_3$, and were used without any further purification. All water used in this study was purified by a Nanopure Infinity Ultrapure water system (Barnstead/Thermolyne, Dubuque, IA) with a minimum resistivity of 18.2 MΩ-cm. The substrates used in the study were hemicylindrical fused silica prisms (Almaz Optics, Marlton, NJ).

Lipid monolayer and bilayer preparation

The LB/LS technique was used to prepare the PSLBs. A 1 mg/ml solution of lipid in $CHCl_3$ was spread at the air/water interface of a Langmuir-Blodgett trough (KSV Instruments, Helsinki, Finland). The first layer was deposited on the substrate via a vertical pull from the aqueous subphase into air. The second layer was deposited on the flat surface of the prism by a horizontal dipping method. The lipid bilayers were maintained in an aqueous environment after deposition. All film transfers were carried out at a surface pressure of 30 mN/m at 22°C (DMPC bilayers were prepared in a cold room at 5°C), corresponding to 42 ± 1.1 Å^2/molecule, 44 ± 1.5 Å^2/molecule, and 46 ± 1.3 Å^2/molecule for DMPC, DPPC, and DSPC, respectively. Asymmetric bilayers were prepared by first depositing a monolayer of the native lipid species followed by the deposition of the perdeuterated analog. Inverted films were prepared by reversing the order of deposition. The samples were transferred to a Teflon flow cell equipped with a type K thermocouple with an accuracy of 0.2°C and a circulating water-jacket for temperature control. The prism and cell were cleaned by submerging them in a solution of 70% 18M sulfuric acid and 30% H_2O_2 for at least 4 h, and then rinsed with copious amounts of Nanopure water (Barnstead/Thermolyne). The prism was then plasma-cleaned for 3 min just prior to use.

SFVS experiments

The SFVS experiments were conducted on a custom-made spectrometer consisting of a tunable IR light source with an optical parametric oscillator (OPO)/optical parametric amplifier (OPA) from LaserVision (Bellevue, WA). The OPO/OPA was pumped with the fundamental output of a Q-switched Nd:YAG laser (Continuum Surelite II, Excel Technology-Continuum Lasers, Santa Clara, CA) generating 1064-nm light at 10 Hz with a pulse duration of 7 ns and an energy of 500 mJ/pulse. Frequency calibration of the OPO was performed using a polystyrene sample. The remainder of the 1064-nm fundamental was frequency-doubled in a potassium titanyl phosphate crystal to generate visible 532-nm light. The IR and 532-nm beams were each collimated to a beam area of ~4 mm^2 and combined on the silica/D_2O interface with incident angles of 72° and 66°, respectively. The IR and visible power intensities used were ~3 mJ/pulse. The sum-frequency signal was filtered with a holographic notch filter (Kaiser Optical, Ann Arbor, MI) and several color filters to remove the residual 532-nm light and then detected with a photomultiplier tube. The signal from the photomultiplier tube was collected with a boxcar integrator (Stanford Research Systems, Sunnyvale, CA). SFVS spectra were obtained by recording the intensity of the sum-frequency response from the surface as a function of the IR frequency. Spectra were acquired at 2 cm^{-1} increments by averaging 100 laser pulses. The kinetic data were obtained by continuously monitoring the CH_3 ν_s intensity at 2875 cm^{-1}. The intensity was averaged for 5-s intervals (50 laser pulses). No additional data processing was performed.

Fluorescence measurements

Fluorescence of the lipid films were collected on an Olympus Bx40 microscope (Olympus, Melville, NY) using a 20× 0.35-NA-long working-distance objective. The sample was excited with a frequency-doubled Nd:YAG laser at 532 nm. The illuminated area was ~0.5 cm^2. Fluorescence micrographs of the lipid films were collected on an Olympus Bx40 microscope with epi-illumination using a 20× 0.35 NA objective.

RESULTS AND DISCUSSION

The integrity of the PSLBs used in this study was verified by both fluorescence microscopy and contact-angle measurements (67). The bilayers were found to be uniform within the resolution of the fluorescence microscope (~1 μm); this, however, does not preclude the possibility of defects smaller than the diffraction limit. Contact-angle measurements revealed a hydrophilic surface consistent with a bilayer structure in which the phosphocholine headgroups are facing outward toward the water phase (67). We have previously examined the SFVS spectra of selectively deuterated DSPC lipids to determine the orientation of the fatty acid lipids chains and phosphocholine headgroup of a PSLB prepared by the LB/LS method (67). Analysis of the vibrational spectra suggests that there is no substantial difference in the structure of the lipids comprising the two leaflets of the bilayer.

The SFVS spectra of the asymmetric lipid bilayers were obtained to identify the vibrational resonances arising from the methyl terminus of the fatty acid chains of the lipids that were used as internal probes to monitor lipid migration. Shown in Fig. 2 are the SFVS spectra of a DMPC/DMPC-d_{67}, DPPC/DPPC-d_{75}, and DSPC/DSPC-d_{83} bilayers in the CH stretching region (2750–3050 cm^{-1}) recorded at 23°C for DSPC and DPPC and 5°C for DMPC. All spectra were collected with *s*-polarized sum-frequency, *s*-polarized visible, and *p*-polarized IR. The water in the sample cell has been replaced with D_2O to eliminate spectral interferences. All three lipid films exhibit nearly identical spectra. The peaks at 2848 cm^{-1} and 2875 cm^{-1} are identified as the CH_2 symmetric stretch (v_s) and CH_3 v_s, respectively, with the shoulder at 2905 cm^{-1} assigned as the CH_2 Fermi resonance. The peak centered at 2950 cm^{-1} is a combination of the CH_3 Fermi resonance (2938 cm^{-1}) and the CH_3 antisymmetric stretch (v_{as}) (2960 cm^{-1}). All resonances are from the fatty acid chains of the lipids (68–71), corroborated by examination of a selectively deuterated lipid sample (DSPC-d_{70}/DSPC-d_{83}) in which only the fatty acid chains have been deuterated (Fig. 2). Indistinguishable spectra were collected for the inverted bilayers DMPC-d_{67}/DMPC, DPPC-d_{75}/DPPC, and DSPC-d_{83}/DSPC, suggesting that the structure of the lipid chains in the upper and lower leaflets of the supported bilayers were nearly identical (J. Liu and J. C. Conboy, unpublished).

To measure the rate of lipid flip-flop, the SFVS CH_3 v_s intensity from the fatty acid chains was measured continuously as a function of time and at various fixed temperatures for the three lipid systems. Several representative decay curves for asymmetrically prepared DMPC/DMPC-d_{67}, DMPC-d_{67}/DMPC, DPPC/DPPC-d_{75}, DPPC-d_{75}/DPPC, DSPC/DSPC-d_{83}, and DSPC-d_{83}/DSPC bilayers are shown in Fig. 3. The CH_3 v_s intensity is seen to decrease with time and the decay rate is highly dependent upon temperature for all three of the lipids examined. As the bilayer structure reaches an equilibrium state, with 50% perdeuterated and 50% perhydrogenated lipids in both layers, the SFVS intensity reaches a minimum. This minimum intensity is the same intensity measured for a premixed 1:1 perdeuterated/perhydrogenated lipid bilayer (63), shown in Fig. 2.

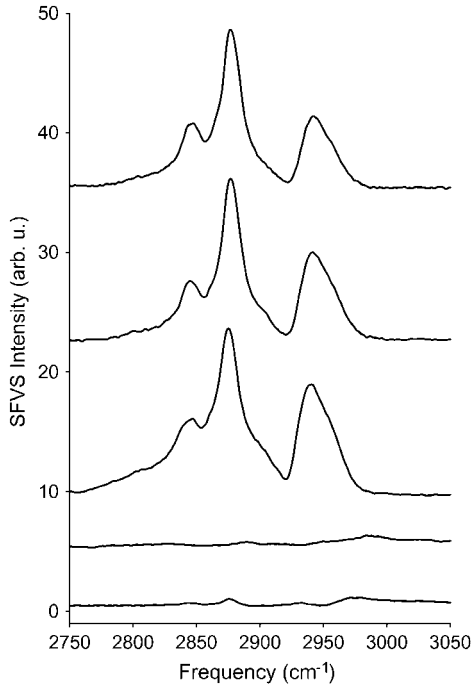

FIGURE 2 From the top to the bottom, SFVS spectra of DMPC/DMPC-d_{67}, DPPC/DPPC-d_{75}, DSPC/DSPC-d_{83}, DSPC-d_{70}/DSPC-d_{83}, and a premixed 1:1 DSPC-d_{83} + DSPC lipid bilayer recorded at 23°C (DMPC/DMPC-d_{67} at 5°C) with *s*-polarized sum-frequency, *s*-polarized visible and *p*-polarized IR.

The SFVS CH_3 v_s intensity is sensitive to the net population inversion of the native lipid species in the bilayer. The intensity of the CH_3 v_s (I_{CH_3}) can be expressed as

$$I_{CH_3} \propto (N_B - N_T)^2, \quad (4)$$

where N_T and N_B are the fraction of the perhydrogenated lipid molecules in the top and bottom leaflets of the lipid bilayer, respectively, with $N_T + N_B = 1$. If a lipid bilayer is assembled such that perdeuterated lipids comprise the bottom leaflet and perhydrogenated lipids are placed in the top leaflet, over time the concentration of native lipids in the upper leaflet will decrease, thereby reducing the asymmetry in the bilayer and reducing the measured CH_3 v_s intensity. This methodology has the advantage that the exchange of

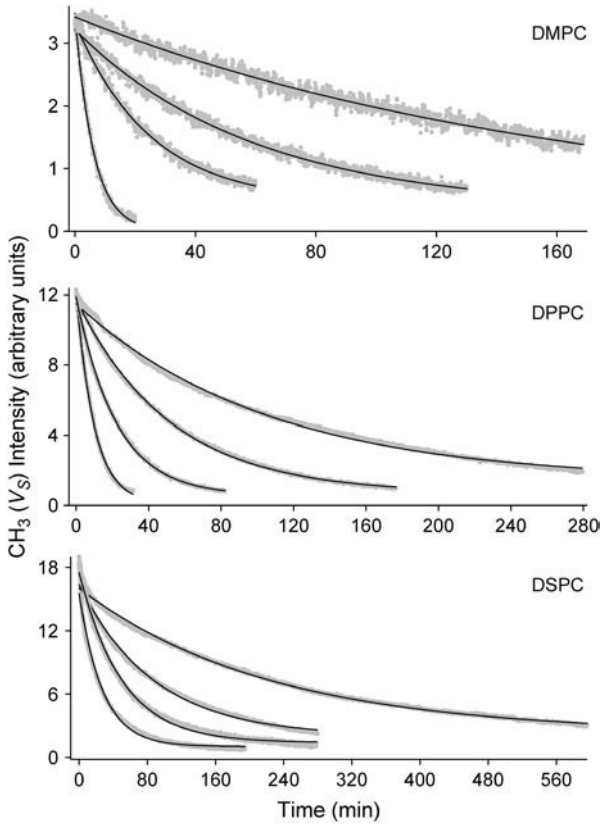

FIGURE 3 CH_3 ν_s intensity decay curves for DMPC/DMPC-d_{67}, DPPC/DPPC-d_{75}, and DSPC/DSPC-d_{83} bilayers (*top* to *bottom*) at various temperatures (DMPC/DMPC-d_{67} at 12.1, 9.8, 7.8, and 4.2°C; DPPC/DPPC-d_{75} at 36.0, 32.3, 29.7, and 27.7°C; and DSPC/DSPC-d_{83} at 50.3, 49.2, 45.7, and 41.7°C from *left* to *right*). All data were collected with *s*-polarized sum-frequency, *s*-polarized visible, and *p*-polarized IR. The solid lines are the fits to the data using Eq. 11.

lipids can be followed using the native lipids themselves. Although it is true that the perdeuterated species have an approximate increase in mass of ~10%, this perturbation is smaller than that introduced by a fluorescence or spin-label. One added advantage of the perdeuterated lipids is that they are chemically identical to the native lipids species. Fluorescence or spin-labeling of lipids considerably alters the chemical identity, resulting in changes in the aqueous solubilities and in some cases the charge on the headgroup.

Kinetics of lipid flip-flop

The kinetics of lipid flip-flop was determined directly from the CH_3 ν_s intensity decay curves shown in Fig. 3. A unimolecular process was assumed for the mechanism, as has been done in previous studies (23,24), which is represented by

$$N_B \underset{k-}{\overset{k+}{\rightleftharpoons}} N_T, \tag{5}$$

with the forward and reverse rate constants given by k_+ and k_-, respectively. If, initially, $N_T = 0$ and $N_B = 1$, with N_B representing the native lipid monolayer in contact with the fused silica substrate, the time-dependent change of N_B is then given by

$$\frac{dN_B}{dt} = k_- N_T - k_+ N_B. \tag{6}$$

When the perdeuterated lipids were placed in either the top or bottom leaflet, identical decay rates were measured within error. This observation suggests that the kinetic rate constants k_+ and k_- are equal. This result also illustrates another important point, namely that the underlying substrate does not appear to be perturbing the dynamics of lipid flip-flop. By equating k_+ to k_- such that $k_+ = k_- = k$, Eq. 6 can then be reduced to

$$\frac{dN_B}{dt} = -k(2N_B - 1). \tag{7}$$

The integrated rate expression is then given by

$$2N_B(t) - 1 = \exp(-2kt), \tag{8}$$

where $2N_B - 1$ is the net population inversion in the bilayer. The SFVS intensity is proportional to the square of the number of molecules on the surface (N); see Eqs. 1 and 3. Since the contribution from opposing lipid molecules is negated, the time-dependent second-order hyperpolarizability, Eq. 2, can be written as

$$\chi^{(2)} = |\chi_R| e^{i\varphi_1} e^{-2kt} + |\chi_{NR}| e^{i\varphi_2}, \tag{9}$$

where $|\chi_R|$ and $|\chi_{NR}|$ are the magnitudes of the complex resonant and nonresonant surface susceptibilities with relative phase angles of φ_1 and φ_2. Substitution of Eq. 9 into Eq. 1 provides an expression for the SFVS signal as a function of time, which is given by

$$I_{CH_3}(t) = I_{R,max} e^{-4kt} + 2\sqrt{I_R}\sqrt{I_{NR}} e^{-2kt} \cos(\theta) + I_{NR} + I_{R,min}, \tag{10}$$

where $I_{R,max}$ and $I_{R,min}$ are the maximum and minimum resonant CH_3 ν_s intensity, I_{NR} is the nonresonant SFVS background, and θ is the phase difference between φ_1 and φ_2. The term $I_{R,min}$ accounts for the nonzero resonance response from the PSLB even after complete lipid exchange has occurred. This has been verified by examining the SFVS spectra of a premixed 1:1 DSPC-d_{83} + DSPC lipid bilayer (Fig. 2), and is most likely due to the asymmetric nature of the interface in which one leaflet is adjacent to the SiO_2 surface and the other is in contact with D_2O (or H_2O). The nonresonant background (I_{NR}), measured independently at 3100 cm^{-1}, which is a spectral region devoid of any C-H resonances, is insignificant and can therefore be eliminated from Eq. 10. As a result, the time-dependent CH_3 ν_s intensity can be simplified as

$$I_{CH_3}(t) = I_{R,max} e^{-4kt} + I_{R,min}. \tag{11}$$

The rate of lipid flip-flop (k) was determined by fitting Eq. 11 to the CH_3 ν_s intensity decays using a nonlinear least-squares

regression in SigmaPlot 9.0 (Systat, Point Richmond, CA), the results of which are shown in Fig. 3. The errors in the rate were determined from the regression analysis. An extremely good correlation between the experimental data and the kinetic model described above is evident.

For comparison, a number of temperature-dependent flip-flop rates obtained from fitting the CH_3 ν_s decay measurements with Eq. 11 are summarized in Table 1. Each value represents a single experiment, with the errors determined from the fits to the data. In addition to the kinetic rate constants, the half-life ($t_{1/2}$) of lipid flip-flop is also tabulated. The $t_{1/2}$, in terms of the rate of lipid flip-flop (Eq. 8), is given by

$$t_{1/2} = \frac{\ln 2}{2k}, \tag{12}$$

which is based on a value of $2N_B(t) - 1 = 0.5$. A comparison of the results shows that there is a substantial increase in the rate of lipid flip-flop as the length of the alkyl chain is reduced from DSPC (C-18) to DMPC (C-14). At ~5°C, below the main phase transition for each lipid, the rates of flip-flop are 196×10^{-5} s^{-1}, 42.2×10^{-5} s^{-1}, and 15.2×10^{-5} for DMPC, DPPC, and DSPC, respectively. It is important to note that all the data summarized in Table 1 were collected below the main phase transition (T_m) of the lipids, which are 23°C, 41°C, and 55°C for DMPC, DPPC, and DSPC, respectively (72). Attempts to measure the rate of lipid exchange near or above T_m were not possible, due to the rapid exchange of lipids at these temperatures.

TABLE 1 Temperature-dependent flip-flop rate constants and $t_{1/2}$ values for DMPC, DPPC, DSPC, and TEMPO-DPPC

	Temperature (°C)	Rate $\kappa \times 10^5 (s^{-1})$	$t_{1/2}$ (min)
DMPC	4.2 ± 0.4	2.56 ± 0.06	226 ± 5
	7.8 ± 0.1	7.04 ± 0.05	82.0 ± 0.6
	9.8 ± 0.1	16.7 ± 0.17	34.6 ± 0.4
	12.1 ± 0.1	68.6 ± 0.87	8.42 ± 0.11
	15.8 ± 0.2	196 ± 5.82	2.95 ± 0.09
	20.4 ± 0.3	443 ± 10.1	1.30 ± 0.03
DPPC	27.7 ± 0.1	3.95 ± 0.02	146 ± 1
	29.7 ± 0.1	8.04 ± 0.02	71.8 ± 0.2
	30.5 ± 0.1	11.6 ± 0.03	49.8 ± 0.1
	31.5 ± 0.1	15.5 ± 0.05	37.3 ± 0.1
	32.3 ± 0.1	18.9 ± 0.07	30.5 ± 0.1
	36.0 ± 0.1	42.2 ± 0.29	13.7 ± 0.1
	36.6 ± 0.1	62.8 ± 0.51	9.20 ± 0.07
DSPC	41.7 ± 0.3	1.85 ± 0.01	312 ± 2
	44.5 ± 0.3	3.60 ± 0.01	160 ± 1
	45.7 ± 0.3	4.67 ± 0.02	124 ± 1
	46.3 ± 0.4	6.72 ± 0.01	86.0 ± 0.1
	49.2 ± 0.2	8.35 ± 0.02	69.2 ± 0.2
	50.3 ± 0.1	15.2 ± 0.06	38.1 ± 0.2
	51.3 ± 0.2	22.3 ± 0.07	25.9 ± 0.1
TEMPO-DPPC	33.1 ± 0.3	0.71 ± 0.08	813 ± 92
	36.1 ± 0.1	0.91 ± 0.12	635 ± 84
	37.0 ± 0.3	1.37 ± 0.24	422 ± 74
	38.3 ± 0.5	1.07 ± 0.13	540 ± 66

The absolute rates of lipid flip-flop measured here are considerably faster than those previously recorded by McConnell for a TEMPO-labeled lipid in egg PC (24), and for fluorescently labeled lipids in similar systems (73). This result is also remarkable because the lipids used in this study were in the gel state below T_m, whereas the lipids used in other studies were principally unsaturated and in the liquid-crystalline phase. It has, however, been suggested that the alteration of the headgroup by the addition of a chromophore or spin-label probe, such as TEMPO, might alter the rates of migration (25). To test this hypothesis, we measured the rate of flip-flop for the spin-labeled lipid TEMPO-DPPC in a DPPC-d_{75} bilayer. TEMPO-DPPC was placed only in the top leaflet at a mole fraction of 0.046 (4.6%) and the SFVS intensity decay from the CH_3 ν_s of the TEMPO lipids was measured as a function of time. The results from the kinetic analysis of the data are listed in Table 1. The rate of interconversion was found to be 0.91×10^{-5} s^{-1} at 36°C ($t_{1/2}$ = 635 min), which is considerably slower than the value obtained from DPPC, which is 42×10^{-5} s^{-1} ($t_{1/2}$ = 13.7 min) at the same temperature. The value for TEMPO-DPPC flip-flop is also approximately five times slower than that measured previously by ESR, from which a rate of $5.0 \times 10^{-5} \pm 1.1 \times 10^{-5}$ s^{-1} at 35°C ($t_{1/2}$ = 116 min) was obtained (24). The slow rate of lipid exchange measured here compared to the previous ESR experiment is most likely the result of the state of the lipid bilayer, gel versus liquid crystalline, used in the two studies. More importantly, however, the kinetic results obtained here suggest that the use of labels can significantly alter the rate of transbilayer movement by an order of magnitude or more.

It has been suggested that the large rates of lipid migration observed by SFVS might be due to desorption of the lipid film from the surface, as SFVS is not capable of distinguishing between lipid flip-flop and the reduction in total lipid content at the surface (74). To rule out this possibility, a fluorescence control experiment was performed in which a PSLB of DPPC was prepared on the same optical substrates used for the SFVS flip-flop measurements, with the addition of 4 mol % NBD-DPPE. The samples were excited with a Nd:YAG laser, similar to that used for the SFVS experiments. The fluorescence intensity was measured as a function of time and illumination rates at 37°C just below the T_m of DPPC, the results of which are shown in Fig. 4 *a*. (37°C is the maximum temperature for which flip-flop kinetics could be reliably measured for DPPC.) Comparison of the results for various time intervals and illumination rates reveals that the decay in the fluorescence intensity is due to photobleaching and not desorption from the surface. When the contributions due to photobleaching are eliminated, Fig. 4 *b*, no apparent desorption from the surface is measured. This result is consistent with previous studies on the stability of PSLBs by fluorescence microscopy, which did not show any appreciable desorption of the film until the temperature was raised much closer to the T_m of the lipid (75). These previous

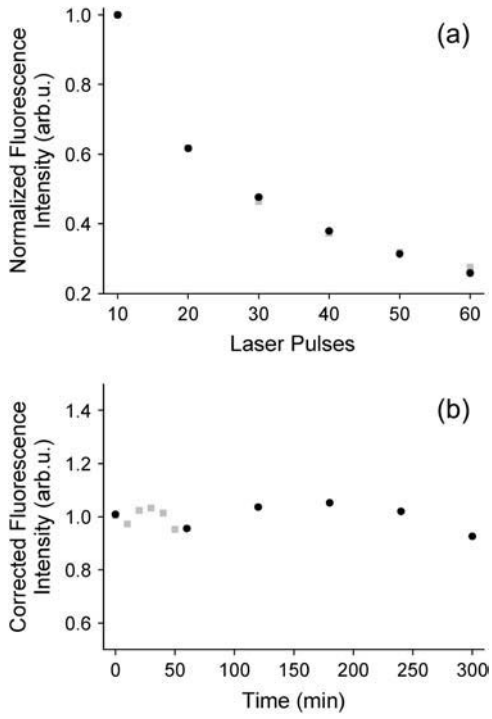

FIGURE 4 Fluorescence measurements of bilayer desorption using 4% NBD-DPPE in a PSLB of DPPC recorded at 37°C. (*a*) Dependence of fluorescence intensity on the number of laser pulses for two different time intervals; one in which the time between sample excitation was 10 min (*shaded squares*) and the other for 60 min (*solid circles*). (*b*) The fluorescence intensity from the bilayer after correcting for photobleaching for both time intervals.

studies also looked at a PSLB which was prepared at a much higher surface pressure (40 mN/m) compared to the films used here (30 mN/m). As a result, the propensity for the film to desorb and form solution phase vesicles should be greatly reduced. It is also important to note that the reproducibility and extremely good signal/noise ratio of the SFVS decays also suggest that the drop in intensity is not a function of lipid desorption from the surface, which would be expected to be far less reproducible and stochastic in nature. We have also previously ruled out heating effects due to the laser on the measured rates of lipid migration (63).

When examining lipid flip-flop in model membrane systems, previous studies have focused primarily on aqueous suspensions of unilamellar vesicles composed of pure lipids (8,23–25) or reconstituted cellular membranes (2,13,15–16). There have also been studies performed on intact cell membranes in vivo (17,18). When performing experiments with PSLBs, some information on the equivalent lateral pressure of a lipid monolayer and a bilayer is needed to make any meaningful correlations with the previously published data. The lateral pressure in a fluid bilayer is believed to range from 30 to 35 mN/m (76). For comparative purposes, the PSLBs used in this study were deposited at a surface pressure of 30 mN/m which provided highly reproducible depositions of DSPC, DPPC, and DMPC. The choice of the lipid surface pressure can affect the resulting dynamics of lipid flip-flop. Our initial analysis of the pressure dependence of DSPC flip-flop suggests that reduction of the lateral surface pressure during deposition by 10 mN/m results in an increase in rate of 1.3 times. If the chosen pressure of 30 mN/m is low compared to that in biological membranes, then we are overestimating the rate of lipid translocation. However, if the lateral pressure in biological membranes is <30 mN/m, the results presented here will underestimate the dynamics of lipid exchange. Unlike liposome systems where the lateral pressure cannot be controlled without exerting significant pressure to the surrounding medium, the pressure in a PSLB is easily controlled by applying a lateral force on the film during deposition, making pressure-dependent measurements more accessible. Studies are ongoing to more fully characterize the effect of the membrane lateral pressure on the thermodynamics and kinetics of lipid translocation.

Activation energy of lipid flip-flop

There have been numerous reports in the literature on the rates of lipid migration in both model and cellular membrane systems. One of the key questions regarding the translocation of lipids which has yet to be fully addressed is: What is the energetic cost or activation barrier to the migration of lipids? For most processes governed by the thermal fluctuations or collisions of molecules, the rate will be dependent upon the activation energy and temperature as described by the Arrhenius equation (77),

$$k = Ae^{-E_a/RT}, \tag{13}$$

where A is the preexponential factor, describing the frequency of events producing products, or in this case translocation of lipids; E_a is the activation energy; T is the temperature; and R is the gas constant. A plot of $ln(k)$ as a function of $1/T$ reveals that the translocation of DMPC, DPPC, and DSPC lipids between leaflets of a PSLB exhibits Arrhenius behavior over the temperature range examined (Fig. 5). The activation energies and preexponential factors calculated from Fig. 5 are listed in Table 2. Activation energies of 230 ± 20, 224 ± 13, and 206 ± 18 kJ/mol were calculated from the data for DMPC, DPPC, and DSPC, respectively. The large activation barrier measured is presumably due to the high energetic cost of moving the hydrophilic headgroup across the hydrophobic membrane core and the energy cost associated with the reorganization of the lipid chains (1). The similarities in activation energies are a reflection of the same transition state for the migration of the hydrated phosphocholine headgroup across the hydrophobic core of the lipid bilayer. This result is not surprising, since the chemical identity of the headgroup is the same for DMPC, DPPC, and DSPC. However, these results suggest that the alkyl chain length does not significantly affect the activation barrier to lipid migration, within the error of the measurement.

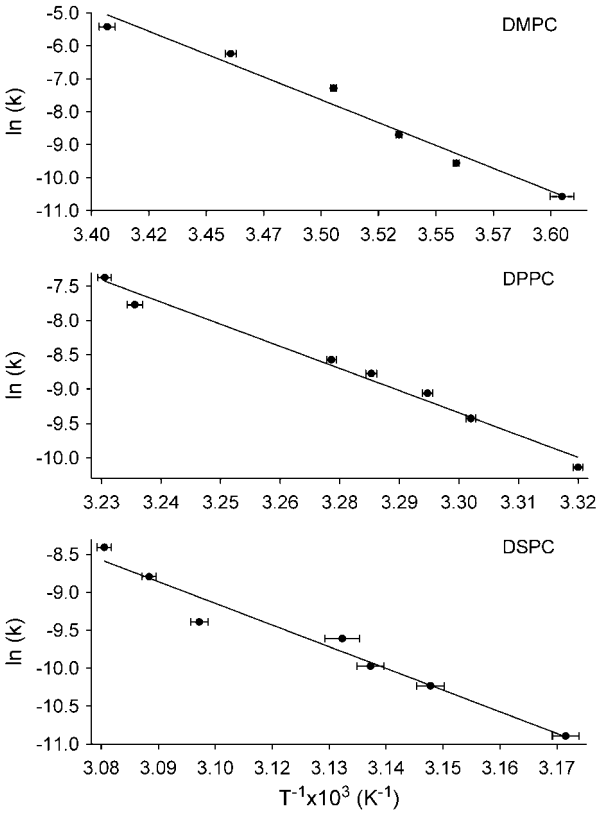

FIGURE 5 Arrhenius plot for DMPC/DMPC-d_{67}, DPPC/DPPC-d_{75}, and DSPC/DSPC-d_{83} using the data in Table 1.

The influence of the fatty acid chain length, however, is seen in the preexponential factor to the Arrhenius equation. The preexponential factor represents the number of successful collisions or in the case of lipid flip-flop, attempted crossings, which lead to lipid inversion. Examination of Table 2 shows a stepwise five-orders-of-magnitude decrease in the preexponential factors among DMPC, DPPC, and DSPC. The strong correlation between the alkyl chain length and A, can be explained as a reduction in the transit time of crossing for the shorter lipids. This hypothesis is consistent with the calculated E_a, in which the chemical environment of the lipid core is maintained; however, the effective width of the barrier to lipid crossing is decreased, leading to larger A values.

From a unimolecular reaction dynamics perspective, the limiting value for the preexponential factor should be $\sim 10^{10}$ to 10^{15} s^{-1}. The values measured here are clearly well beyond that described by a simple unimolecular process. It is important to note the large error in the calculated preexponential factors, which is a consequence of the limited temperature range over which accurate measurements can be obtained as well as the scatter in the measured rates. However, the observation of non-Arrhenius behavior, as suggested by the large preexponential factors, is not uncommon. Similar activation energies and preexponential factors have been measured for the dissociation of proteins and protein-ligand complexes in the gas phase, which has been attributed to the softening of a large number of librational modes during the course of the reaction (78). It is also possible that the change in heat capacity near the transition state of the lipids may be convolved with the thermodynamics of lipid flip-flop, thereby altering the measured E_a and A. The results of the Arrhenius analysis suggest that although a linear relationship exists between $ln(k)$ and $1/T$, these results can only be used to provide an effective activation energy over the temperature range examined.

The activation energy and preexponential factors calculated for DMPC, DPPC, and DSPC are also considerably higher than those previously determined by McConnell, who measured an activation energy of ~81 kJ/mol for TEMPO-DPPC in an egg PC matrix with a frequency factor of 2.72×10^9 s^{-1} (24). A summation of the SFVS kinetic data for TEMPO-DPPC can be seen in the Arrhenius plot of Fig. 6. The scatter in the data is a consequence of the much lower signal/noise which is a consequence of the low concentration of CH_3 groups in the bilayer. For the TEMPO experiments, there are only ~5% CH_3 groups in the bilayer, which represents an order-of-magnitude decrease in the measured response compared to DPPC. An activation energy of 79 ± 42 kJ/mol and a preexponential factor of 2.3×10^8 s^{-1} were calculated. These results compare favorably with those previously measured by McConnell. However, care must be taken in making too strong a correlation between the

TABLE 2 Lipid flip-flop activation energies (E_a) and preexponential factors (A) for DMPC, DPPC, DSPC, and TEMPO-DPPC

	E_a (kJ/mol)	A (s^{-1})
DMPC	230 ± 20	$6.4 \times 10^{38} \pm 6.1 \times 10^{37}$
DPPC	224 ± 13	$3.4 \times 10^{34} \pm 2.1 \times 10^{33}$
DSPC	206 ± 18	$3.6 \times 10^{29} \pm 3.7 \times 10^{28}$
TEMPO-DPPC	79 ± 42	$2.3 \times 10^{8} \pm 2.0 \times 10^{8}$

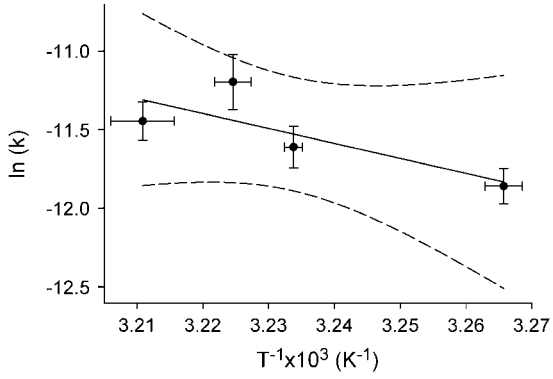

FIGURE 6 Arrhenius plot for TEMPO-DPPC in a DPPC-d_{75} bilayer using the data in Table 1. The dashed lines represent the 95% confidence interval derived from the fit of the data.

previous ESR data and the SFVS results presented here, because of the large errors in the measured kinetic rates from both experiments. One possible reason for the lower E_a and A measured for TEMPO-DPPC versus DPPC may lie in the fact that there is a low concentration of the lipid probe in the membrane. If lipid flip-flop involves a concerted motion of the lipids in the membrane, as suggested by the SFVS data for DMPC, DPPC, and DSPC, the absence of lipid-lipid correlation may account for the reduced rate and lower E_a and A. It is also possible that the more hydrophobic character of the TEMPO-labeled headgroup also facilitates the transfer of the lipid through the membrane.

CONCLUSIONS

The results presented here demonstrate the unique attributes of SFVS and the use of PSLBs for the investigation of lipid flip-flop in PSLBs. By using deuterated lipid analogs, no chemical or structural modifications are performed to the lipids under investigation. The use of PSLBs for the measurement of lipid flip-flop also allows for direct control over the composition and physical properties of the membrane, without the need of chemical modification to the lipid bilayer. The rate of flip-flop for DMPC, DPPC, and DSPC was found to range from 196×10^{-5} s^{-1}, 42.2×10^{-5} s^{-1} to 15.2×10^{-5} s^{-1}, at 5°C below the main phase transition temperature of the lipids. The rate of translocation was too fast to measure near or above the main phase-transition temperature of the lipids studied. These results have important implications for understanding the transbilayer movement of lipids in biological membranes. Cellular membranes are composed of a vast array of lipid species with a broad range of transition temperatures. Based on our preliminary findings, the migration of certain lipid species in living cells could be quite facile under physiological conditions in the absence of a protein-mediated process. The kinetics of lipid flip-flop exhibited Arrhenius behavior with a calculated activation energy of ~220 kJ/mol for DMPC, DPPC, and DSPC. A large variation was seen in the preexponential factor which varied stepwise by five orders of magnitude among DMPC, DPPC, and DSPC, and accounts for the wide spread in kinetic rates measured for this series of lipids. The preexponential factors measured were considerably higher than those typically encountered for a unimolecular reaction, suggesting non-Arrhenius behavior.

In addition to the kinetics of the native lipid species, the influence of lipid labeling was also examined. The addition of the TEMPO label to DPPC significantly altered its measured rate, reducing it by an order of magnitude compared to DPPC. The activation energy and preexponential factor measured for TEMPO-DPPC were found to be comparable to that previously measured by ESR, but considerably lower than DPPC. These experiments demonstrate the effect lipid labeling can have on the measured rate of lipid migration. The chemical and structural modifications of the lipids can have dramatic effects on the thermodynamics and kinetics of lipid translocation in model membrane systems. These studies are being extended to examine the effect of lipid composition, as well as the influence of proteins and cholesterol on lipid flip-flop.

The authors thank the reviewers of this manuscript for their comments and suggestions.

This work was supported by funds from the National Institutes of Health (grant No. GM068120-01).

REFERENCES

1. Kol, M. A., B. de Kruijff, and A. I. P. M. de Kroon. 2002. Phospholipid flip-flop in biogenic membranes: what is needed to connect opposite sides. *Semin. Cell Dev. Biol.* 13:163–170.
2. Buton, X., G. Morrot, P. Fellmann, and M. Seigneuret. 1996. Ultra-fast glycerophospholipid selective transbilayer motion mediated by a protein in the endoplasmic reticulum membrane. *J. Biol. Chem.* 271:6651–6658.
3. Herrmann, A., A. Zachowski, and P. F. Devaux. 1990. Protein mediated phospholipid translocation in the endoplasmic reticulum with a low lipid specificity. *Biochemistry.* 29:2023–2027.
4. Martin, O. C., and R. E. Pagano. 1987. Transbilayer movement of fluorescent analogs of phosphatidylserine and phosphatidylethanolamine at the plasma membrane of cultured cells. Evidence for a protein-mediated and ATP-dependent process(es). *J. Biol. Chem.* 262:5890–5898.
5. Eytan, G. D., R. Regev, G. Oren, and Y. G. Assaraf. 1996. The role of passive transbilayer drug movement in multidrug resistance and its modulation. *J. Biol. Chem.* 271:12897–12902.
6. Balasubramanian, K., and C. M. Gupta. 1996. Transbilayer phosphatidylethanolamine movements in the yeast plasma membrane. Evidence for a protein-mediated, energy-dependent mechanism. *Eur. J. Biochem.* 240:798–806.
7. Margolles, A., M. Putman, H. W. van Veen, and W. N. Konings. 1999. The purified and functionally reconstituted multidrug transporter LMRA of *Lactococcus lactis* mediates the transbilayer movement of specific fluorescent phospholipids. *Biochemistry.* 38:16298–16306.
8. Kol, M. A., A. N. C. van Laak, D. T. S. Rijkers, J. A. Killian, A. I. P. M. de Kroon, and B. de Kruijff. 2003. Phospholipid flop induced by transmembrane peptides in model membranes is modulated by lipid composition. *Biochemistry.* 42:231–237.
9. Hrafnsdottir, S., J. W. Nichols, and A. K. Menon. 1997. Transbilayer movement of fluorescent phospholipids in *Bacillus megasterium* membrane vesicles. *Biochemistry.* 36:4969–4978.
10. Fattal, E., S. Nir, R. A. Parente, and F. C. Szoka, Jr. 1994. Pore-forming peptides induce rapid phospholipid flip-flop in membranes. *Biochemistry.* 33:6721–6731.
11. Schwichtenhoevel, C., B. Deuticke, and C. W. M. Haest. 1992. Alcohols produce reversible and irreversible acceleration of phospholipid flip-flop in the human erythrocyte membrane. *Biochim. Biophys. Acta.* 1111:35–44.
12. Bishop, W., and R. Bell. 1985. Assembly of the endoplasmic reticulum phospholipid bilayer: the phosphatidylcholine transporter. *Cell.* 42: 51–60.
13. Devaux, P. F. 1993. Phospholipid translocation in the endoplasmic reticulum. *In* Subcellular Biochemistry: Endoplasmic Reticulum, Vol. 21. N. Borgese and J.R. Haris, editors. Plenum Press, London. 273–285.
14. Marx, U., G. Lassmann, H. G. Holzhutter, D. Wustner, P. Muller, A. Hohlig, J. Kubelt, and A. Herrmann. 2000. Rapid flip-flop of phospholipids in endoplasmic reticulum membranes studied by a stopped-flow approach. *Biophys. J.* 78:2628–2640.

15. Devaux, P. F., and A. Zachowski. 1994. Maintenance and consequences of membrane phospholipid asymmetry. *Chem. Phys. Lipids.* 73:107–120.

16. Menon, A. K., W. E. Watkins III, and S. Hrafnsdottir. 2000. Specific proteins are required to translocate phosphatidylcholine bidirectionally across the endoplasmic reticulum. *Curr. Biol.* 10:241–252.

17. Bolhuis, H., H. W. van Veen, D. Molenaar, B. Poolman, A. J. M. Driessen, and W. N. Konings. 1996. Multidrug resistance in *Lactococcus lactis*: evidence for ATP-dependent drug extrusion from the inner leaflet of the cytoplasmic membrane. *EMBO J.* 15:4239–4245.

18. Gummadi, S. N., S. Hrafnsdottir, J. Walent, W. E. Watkins, and A. K. Menon. 2003. Reconstitution and assay of biogenic membrane-derived phospholipid flippase activity in proteoliposomes. *Methods Mol. Biol.* 228:271–279.

19. Pomorski, T., P. Muller, B. Zimmermann, K. Burger, P. F. Devaux, and A. Herrmann. 1996. Transbilayer movement of fluorescent and spin-labeled phospholipids in the plasma membrane of human fibroblasts: a quantitative approach. *J. Cell Sci.* 109:687–698.

20. Raggers, R. J., T. Pomorski, J. C. M. Holthuis, N. Kalin, and G. Van Meer. 2000. Lipid traffic: the ABC of transbilayer movement. *Traffic* (*Copenhagen*). 1:226–234.

21. Zachowski, A. 1993. Phospholipids in animal eukaryotic membranes: transverse asymmetry and movements. *Biochem. J.* 294:1–14.

22. Menon, A. K. 1995. Flippases. *Trends Cell Biol.* 5:355–360.

23. John, K., S. Schreier, J. Kubelt, A. Herrmann, and P. Muller. 2002. Transbilayer movement of phospholipids at the main phase transition of lipid membranes: implications for rapid flip-flip in biological membranes. *Biophys. J.* 83:3315–3323.

24. Kornberg, R. D., and H. M. McConnell. 1971. Inside-outside translocation of phospholipids in vesicle membranes. *Biochemistry.* 10: 1111–1120.

25. Devaux, P. F., P. Fellmann, and P. Herve. 2002. Investigation on lipid asymmetry using lipid probes comparison between spin-labeled lipids and fluorescent lipids. *Chem. Phys. Lipids.* 116:115–134.

26. Frasch, S. C., P. M. Henson, K. Nagaosa, M. B. Fessler, N. Borregaard, and D. L. Bratton. 2004. Phospholipid flip-flop and phospholipid scramblase 1 (PLSCR1) co-localize to uropod rafts in formylated Met-Leu-Phe-stimulated neutrophils. *J. Biol. Chem.* 279:17625–17633.

27. Dolis, D., A. I. P. M. de Kroon, and B. de Kruijff. 1996. Transmembrane movement of phosphatidylcholine in mitochondrial outer membrane vesicles. *J. Biol. Chem.* 34:11879–11883.

28. Fattal, E., R. A. Parente, S. Nir, and F. C. Szoka, Jr. 1992. Phospholipid flip-flop induced by membrane-associated peptides. *Congr. Int. Technol. Pharm. 6th.* 5:70–81.

29. McIntyre, J. C., and R. G. Sleight. 1991. Fluorescence assay for phospholipid membrane asymmetry. *Biochemistry.* 30:11819–11827.

30. McNamee, M. G. 1973. Transmembrane potentials and phospholipids flip-flop in excitable membrane vesicles. *Diss. Abstr. Int. B.* 34:2547.

31. Anzai, K., Y. Yoshioka, and Y. Kirino. 1993. Novel radioactive phospholipid probes as a tool for measurement of phospholipid translocation across biomembranes. *Biochim. Biophys. Acta.* 1151:69–75.

32. McNamee, M. G., and H. M. McConnell. 1973. Transmembrane potentials and phospholipid flip-flop in excitable membrane vesicles. *Biochemistry.* 12:2951–2958.

33. Verhallen, P. F. J., P. Comfurius, E. M. Bevers, A. J. W. G. Visser, and R. F. A. Zwaal. 1988. Cytoskeletal degradation by calpain results in ''flip flop'' of phosphatidylserine in the plasma membrane of activated blood platelets. *Colloq. INSERM.* 171:307–312.

34. Fellmann, P., P. Herve, and P. F. Devaux. 1993. Transmembrane distribution and translocation of spin-labeled plasmalogens in human red blood cells. *Chem. Phys. Lipids.* 66:225–230.

35. Gallet, P. F., A. Zachowski, P. Fellmann, R. Julien, P. F. Devaux, and A. Maftah. 1999. Transbilayer movement and distribution of spin-labeled phospholipids in the inner mitochondrial membrane. *Biochim. Biophys. Acta.* 1418:61–70.

36. Rousselet, A., A. Colbeau, P. M. Vignais, and P. F. Devaux. 1976. Study of the transverse diffusion of spin-labeled phospholipids in biological membranes. II. Inner mitochondrial membrane of rat liver: use of phosphatidylcholine exchange protein. *Biochim. Biophys. Acta.* 426: 372–384.

37. Grant, A. M., P. K. Hanson, L. Malone, and J. W. Nichols. 2001. NBD-labeled phosphatidylcholine and phosphatidylethanolamine are internalized by transbilayer transport across the yeast plasma membrane. *Traffic.* 2:37–50.

38. Boon, J. M., and B. D. Smith. 2001. Facilitated phosphatidylcholine flip-flop across erythrocyte membranes using low molecular weight synthetic translocases. *J. Am. Chem. Soc.* 123:6221–6226.

39. Colleau, M., P. Herve, P. Fellmann, and P. F. Devaux. 1991. Transmembrane diffusion of fluorescent phospholipids in human erythrocytes. *Chem. Phys. Lipids.* 57:29–37.

40. Dekkers, D. W. C., P. Comfurius, A. J. Schroit, E. M. Bevers, and R. F. A. Zwaal. 1998. Transbilayer movement of NBD-labeled phospholipids in red blood cell membranes: outward-directed transport by the multidrug resistance protein 1 (MRP1). *Biochemistry.* 37:14833–14837.

41. Haldar, K., A. F. De Amorim, and G. A. M. Cross. 1989. Transport of fluorescent phospholipid analogs from the erythrocyte membrane to the parasite in *Plasmodium falciparum*-infected cells. *J. Cell Biol.* 108:2183–2192.

42. Kitagawa, S., and M. Takegaki. 1992. Transbilayer incorporation of 1-pyrenebutyltrimethylammonium by blood platelets and its application for analyzing changes in physico-chemical properties of the membrane lipid bilayer induced by platelet activation. *Biochim. Biophys. Acta.* 1107:231–237.

43. Kitagawa, S. 1998. Asymmetry of fluidity of biological membrane and drug transport. *Yakugaku Kenkyu no Shinpo.* 14:45–53.

44. Wolf, D. E., A. P. Winiski, A. E. R. Ting, K. M. Bocian, and R. E. Pagano. 1992. Determination of the transbilayer distribution of fluorescent lipid analogs by non-radiative fluorescence resonance energy transfer. *Biochemistry.* 31:2856–2873.

45. Sleight, R. G., and R. E. Pagano. 1984. Transport of a fluorescent phosphatidylcholine analog from the plasma membrane to the Golgi apparatus. *J. Cell Biol.* 99:742–751.

46. McConnell, H. M., T. H. Watts, R. M. Weis, and A. A. Brian. 1986. Supported planar membranes in studies of cell-cell recognition in the immune system. *Biochim. Biophys. Acta.* 864:95–106.

47. Thompson, N. L., and A. G. Palmer III. 1988. Model cell membranes on planar substrates. *Comments Mol. Cell. Biophys.* 5:39–56.

48. Crane, J. M., and L. K. Tamm. 2004. Role of cholesterol in the formation and nature of lipid rafts in planar and spherical model membranes. *Biophys. J.* 86:2965–2979.

49. Ottova, A. L., and H. T. Tien. 2003. Supported planar BLMs (lipid bilayers). Formation, methods of study, and applications. *In* Interfacial Catalysis. Marcel Dekker, New York. 421–459.

50. Trojanowicz, M. 2003. Analytical applications of planar bilayers lipid membranes. *Membr. Sci. Technol.* 7:807–845.

51. Slade, A., J. Luh, S. Ho, and C. M. Yip. 2002. Single molecule imaging of supported planar lipid bilayer-reconstituted human insulin receptors by in situ scanning probe microscopy. *J. Struct. Biol.* 137: 283–291.

52. Conboy, J. C., K. D. McReynolds, J. Gervay-Hague, and S. S. Saavedra. 2002. Quantitative measurements of recombinant HIV surface glycoprotein 120 binding to several glycosphingolipids expressed in planar supported lipid bilayers. *J. Am. Chem. Soc.* 124: 968–977.

53. Ottova, A. L., and H. T. Tien. 2000. Supported planar lipid bilayers (BLMs) as biosensors. *J. Surf. Sci. Technol.* 16:115–148.

54. Dietrich, C., L. A. Bagatolli, Z. N. Volovyk, N. L. Thompson, M. Levi, K. Jacobson, and E. Gratton. 2001. Lipid rafts reconstituted in model membranes. *Biophys. J.* 80:1417–1428.

55. Plant, A. L. 1999. Supported hybrid bilayer membranes as rugged cell membrane mimics. *Langmuir.* 15:5128–5135.

56. Cremer, P. S., and S. G. Boxer. 1999. Formation and spreading of lipid bilayers on planar glass supports. *J. Phys. Chem. B.* 103:2554–2559.

57. Conboy, J. C., S. Liu, D. F. O'Brien, and S. S. Saavedra. 2003. Planar supported bilayer polymers formed from bis-diene lipids by Langmuir-Blodgett deposition and UV irradiation. *Biomacromolecules.* 4:841–849.

58. Starr, T. E., and N. L. Thompson. 2000. Formation and characterization of planar phospholipid bilayers supported on TiO_2 and $SrTiO_3$ single crystals. *Langmuir.* 16:10301–10308.

59. Leonenko, Z. V., A. Carnini, and D. T. Cramb. 2000. Supported planar bilayer formation by vesicle fusion: the interaction of phospholipid vesicles with surfaces and the effect of gramicidin on bilayer properties using atomic force microscopy. *Biochim. Biophys. Acta.* 1509:131–147.

60. Nollert, P., H. Kiefer, and F. Jaehnig. 1995. Lipid vesicle adsorption versus formation of planar bilayers on solid surfaces. *Biophys. J.* 69: 1447–1455.

61. Kalb, E., S. Frey, and L. K. Tamm. 1992. Formation of supported planar bilayers by fusion of vesicles to supported phospholipid monolayers. *Biochim. Biophys. Acta.* 1103:307–316.

62. Wagner, M. L., and L. K. Tamm. 2000. Tethered polymer-supported planar lipid bilayers for reconstitution of integral membrane proteins: silane-polyethyleneglycol-lipid as a cushion and covalent linker. *Biophys. J.* 79:1400–1414.

63. Liu, J., and J. C. Conboy. 2004. Direct measurement of the transbilayer movement of phospholipids by sum-frequency vibrational spectroscopy. *J. Am. Chem. Soc.* 126:8376–8377.

64. Shen, Y. R. 1984. The Principles of Nonlinear Optics. Wiley, New York.

65. Guyot-Sionnest, P., Y. R. Shen, and T. F. Heinz. 1987. Determination of the nonlinear optical susceptibility of surface layers. *Appl. Phys. B.* 42:237–238.

66. Dick, B., A. Gierulski, G. Marowsky, and G. A. Reider. 1985. Determination of the nonlinear optical susceptibility χ^2 of surface layers by sum and difference frequency generation in reflection and transmission. *Appl. Phys. B.* B38:107–116.

67. Lui, J., and J. C. Conboy. 2005. Structure of a gel phase lipid bilayer prepared by the Langmuir-Blodgett/Langmuir-Schaefer method characterized by sum-frequency vibrational spectroscopy. *Langmuir.* In press.

68. Conboy, J. C., M. C. Messmer, and G. L. Richmond. 1997. Dependence of alkyl chain conformation of simple ionic surfactants on head group functionality as studied by vibrational sum-frequency spectroscopy. *J. Phys. Chem. B.* 101:6724–6733.

69. Conboy, J. C., M. C. Messmer, and G. L. Richmond. 1998. Effect of alkyl chain length on the conformation and order of simple ionic surfactants adsorbed at the D_2O/CCl_4 interface as studied by sum-frequency vibrational spectroscopy. *Langmuir.* 14:6722–6727.

70. Conboy, J. C., M. C. Messmer, and G. L. Richmond. 1996. Investigation of surfactant conformation and order at the liquid-liquid interface by total internal reflection sum-frequency vibrational spectroscopy. *J. Phys. Chem.* 100:7617–7622.

71. Walker, R. A., J. C. Conboy, and G. L. Richmond. 1997. Molecular structure and ordering of phospholipids at a liquid-liquid interface. *Langmuir.* 13:3070–3073.

72. Koynova, R., and M. Caffrey. 1998. Phases and phase transitions of the phosphatidylcholines. *Biochim. Biophys. Acta.* 1376:91–145.

73. Abreu, M. S. C., M. J. Moreno, and W. L. C. Vaz. 2004. Kinetics and thermodynamics of association of a phospholipid derivative with lipid bilayers in liquid-disordered and liquid-ordered phases. *Biophys. J.* 87:353–365.

74. Crane, J. M., V. Kiessling, and L. K. Tamm. 2005. Measuring lipid asymmetry in planar supported bilayers by fluorescence interference contrast microscopy. *Langmuir.* 21:1377–1388.

75. Tamm, L. K., and H. M. McConnell. 1985. Supported phospholipid bilayers. *Biophys. J.* 47:105–113.

76. Marsh, D. 1996. Lateral pressure in membranes. *Biochim. Biophys. Acta.* 1286:183–223.

77. Atkins, P. W. 1990. Physical Chemistry, 4th Ed. W.H. Freeman and Company, New York.

78. Laskin, J., and J. H. Futrell. 2003. Entropy is the major driving force for fragmentation of proteins and protein-ligand complexes in the gas phase. *J. Phys. Chem. A.* 107:5836–5839.